

Kinetic turbulence in space plasmas observed in the near-Earth and near-Sun solar wind.

Olga Alexandrova¹, Vamsee Jagarlamudi^{2,1}, Claudia Rossi¹,
Milan Maksimovic¹, Petr Hellinger^{3,4}, Yuri Shprits⁵, & Andre Mangeney¹

¹*LESIA, Observatoire de Paris, Université PSL, CNRS, Sorbonne Université,
Université de Paris, 5 place Jules Janssen, 92195 Meudon, France.*

²*LPC2E, CNRS, University of Orléans, 3 Avenue de la Recherche Scientifique, 45071 Orleans Cedex 2, France.*

³*Astronomical Institute, CAS, Bocni II/1401, Prague CZ-14100, Czech Republic*

⁴*Institute of Atmospheric Physics, CAS, Bocni II/1401, Prague CZ-14100, Czech Republic and*

⁵*GFZ German Research Centre for Geosciences, University of Potsdam, Germany.*

(Dated: March 2, 2020)

Turbulence develops in any stressed flow when the scales of the forcing are much larger than those of the dissipation. In neutral fluids, it consists of chaotic motions in physical space but with a universal energy spectrum in Fourier space. Intermittency (non-Gaussian statistics of fluctuations) is another general property and it is related to the presence of coherent structures. Space plasmas are turbulent as well. Here, we focus on the kinetic plasma scales, which are not yet well understood. We address the following fundamental questions: (1) Do the turbulent fluctuations at kinetic scales form a universal spectrum? and (2) What is the nature of the fluctuations? Using measurements in the solar wind we show that the magnetic spectra of kinetic turbulence at 0.3, 0.6 and 0.9 AU from the Sun have the same shape as the ones close to the Earth orbit at 1 AU, indicating universality of the phenomenon. The fluctuations, which form this spectrum, are typically non-linearly interacting eddies that tend to generate magnetic filaments.

I. CURRENT STATE OF THE FIELD AND LONG-STANDING QUESTIONS

Turbulence is one of the unsolved problems in physics: to date, there is no satisfactory theory, based on first principles, that describes turbulence in a sufficiently general frame. Therefore, one has to rely on phenomenologies. For example, the observed general spectrum of the inertial range of the incompressible neutral fluid turbulence $\sim k^{-5/3}$ (with wavenumber k) is well described by Kolomogorov's phenomenology [33]. Intermittency (or non-Gaussianity of fluctuations and their dependency on scale) is beyond this description, and in neutral fluids it is due to coherent structures like filaments of vorticity. Their cross section is of the order of the dissipation scale ℓ_d . The dissipation range is described by another general law $\sim k^{-3} \exp(-Ck\ell_d)$, with C being a constant close to 7 [15]. Such a spectrum with an exponential correction indicates a lack of self-similarity in the dissipation range where turbulent energy is transferred into heat.

Astrophysical plasmas differ from usual neutral fluids. Natural plasmas (i) are almost collisionless so that the viscosity and Kolomogorov's dissipation scale ℓ_d are ill-defined; (ii) are almost completely ionized so that the presence of a magnetic field will introduce an anisotropy and allow waves to propagate, even in the incompressible limit (Alfvén waves); (iii) are characterized by a number of characteristic plasma (or kinetic) scales; (iv) are dispersive: beyond Alfvén waves, one may also expect fast and/or slow magnetosonic waves at magnetohydrodynamic (MHD) scales, and, at kinetic scales, kinetic Alfvén, whistler or slow/ion-acoustic waves, etc...

Considering all this complexity, one may wonder if there is a certain degree of generality in space plasma

turbulence. If this is the case, are there similarities with incompressible neutral fluid turbulence? To answer these questions, the solar wind plasma, which is accessible to in-situ space exploration, has proven to be a very useful laboratory. However, it is inhomogeneous, with a dense slow wind blowing at low heliographic latitudes and a fast and more tenuous wind at high latitudes; it is also in spherical expansion, so that some extra complexity is added: in particular the particle distribution functions tend to develop strong anisotropies and become unstable, generating fluctuations at small, kinetic scales.

Since the first early in-situ measurements, [e.g., 16], our knowledge of the large-scale turbulence in the solar wind has greatly improved, [e.g., 11, 32]. There is an extended inertial range of scales, where incompressible MHD phenomenologies [9, 14, 22], similar in spirit to the Kolomogorov's phenomenology, may be invoked to understand the formation of a Kolmogorov-like spectrum of magnetic fluctuations $\sim k^{-5/3}$ [44]. At the short wavelength end of the inertial domain, i.e., at scales of the order of the ion inertial scale $\lambda_p = c/\omega_{pp}$ (where c is the speed of light and ω_{pp} is the proton plasma frequency) the spectrum steepens. At these scales (~ 100 km at 1 AU), the MHD approximation is no longer valid; the "heavy" ion (basically proton in the solar wind) fluid and the "light" electron fluid behave separately, [e.g., 26, 40, 46]. At even smaller scales, at the vicinity of the electron scales (~ 1 km at 1 AU), the fluid description does not hold any more and electrons should be considered as particles. The present paper is concerned with this short wavelength range, i.e., between ion scales and a fraction of electron scales.

Recently, thanks to a very sensitive Search Coil Magnetometer on the ESA/Cluster mission [17, 19], the small scale tail of the electromagnetic cascade could be ex-

ploded down to electron scales, i.e., the electron inertial length $\lambda_e = c/\omega_{ep}$ (where ω_{ep} is the electron plasma frequency), the electron Larmor radius $\rho_e = V_{e\perp}/\omega_{ce}$ (where $V_{e\perp} = \sqrt{2kT_{e\perp}/m_e}$ is the electron thermal speed in the plane perpendicular to the mean magnetic field \mathbf{B}_0 , $T_{e\perp}$ is the perpendicular to \mathbf{B}_0 electron temperature, m_e is the mass of electron and $\omega_{ce} = 2\pi f_{ce}$ is the electron cyclotron frequency) and below ($\sim 0.2 - 1$ km) [2–4, 54, 55].

The Cluster mission operates at 1 AU, and provides observations which seem confusing at first glance. At electron scales, the spectral shape of the magnetic fluctuations vary from event to event suggesting that the spectrum is not universal at kinetic scales [54, 55]. However, it may be shown [53] that most of these spectral variations are due to the presence or absence of whistler waves with frequencies of a fraction of f_{ce} and wave vectors \mathbf{k} quasi-parallel to \mathbf{B}_0 [35]. These waves may result from the development of some instabilities associated either to an increase of the electron temperature anisotropy or an increase of the electron heat flux, in some regions of the solar wind [57].

Are whistler waves part of the background turbulence at kinetic scales? Turbulent fluctuations at these scales have low frequencies in the plasma frame ($f \simeq 0$) and wave-vectors mostly perpendicular to the mean field $\mathbf{k} \perp \mathbf{B}_0$ [36]. This background turbulence is convected by the solar wind (with the speed \mathbf{V}) across the spacecraft and appears in the satellite frame at frequencies $f = k_{\perp}V/2\pi$. It happens that these frequencies are below but close to f_{ce} , exactly in the range where whistler waves (with $\mathbf{k} \parallel \mathbf{B}_0$ and $f \leq f_{ce}$) may appear locally. Therefore, the superposition of turbulence and whistlers at the same frequencies is incidental. If we could do measurements directly in the plasma frame, these two phenomena would be completely separated in \mathbf{k} and f . A possible interaction between turbulence and whistlers is out of the scope of the present paper. We focus here on the background turbulence at kinetic scales only.

A statistical study of solar wind streams at 1 AU under different plasma conditions has shown that, in absence of whistler waves, the turbulent spectrum seems to follow a general shape $\sim f^{-8/3} \exp(-f/f_d)$ [3]. The characteristic frequency f_d is strongly correlated with the Doppler-shifted electron Larmor radius $f_{\rho_e} = V/(2\pi\rho_e)$ [2, 3], and, by analogy with the neutral fluid case, it is referred here to as the “dissipation frequency”, associated with a local “dissipation scale” $\ell_d = V/(2\pi f_d)$.

Two basic questions arise. First question: how general is the kinetic spectrum, observed at 1 AU [3]? Intuitively, one may think that turbulent fluctuations at such small scales are well mixed, showing the same spectrum at any radial distance from the Sun, except for the temporary excitation of whistler waves. We address this question in section II, where we analyse the data from Helios, the first mission which explored the inner Heliosphere up to the orbit of Mercury (0.3 AU). Helios provided magnetic spectra up to the electron scales at radial distances

0.3 – 1 AU [18]. These measurements have shown that the mean magnetic spectrum at 0.3 AU follows a power-law $\sim f^{-3}$ between ion and electron scales, but a global and systematic analysis of the spectral behaviour of the magnetic field fluctuations over the whole accessible scale range is still lacking, except at 1 AU. We present an analysis of more than 240 000 available magnetic spectra of kinetic turbulence in the inner Heliosphere obtained by Helios-1 in three distance range: around 0.3, 0.6 and 0.9 AU. We show that these spectra follow the general shape previously observed at 1 AU [3].

Second question: what is the nature of fluctuations at kinetic scales? *Weak* (or *wave*) turbulence implies a mixture of small amplitude *weakly interacting random phase waves*, which follow a particular dispersion relation. In the case of weak turbulence, the dissipation is homogeneous in space and is due to collisionless dissipation of waves, such as Landau damping, [e.g., 37]. Since, the amplitudes of fluctuations at kinetic scales are small in the solar wind, the wave turbulence scenario is frequently assumed; but an unambiguous identification of the type of waves (and the corresponding dispersion relation) in the kinetic range remains elusive, despite a vast amount of work encompassing theory, simulations and observations aimed at resolving this ‘wave-debate, [e.g., 12, 13, 18, 21, 41, 51, 54]. On the other hand, *strong turbulence* implies non-linearly interacting eddies leading to the generation of coherent structures (energetic events with coupled phases across a wide range of scales). Then, the dissipation is non-homogeneous in space and concentrates within or near coherent structures.

We address the second question in section III. Using Cluster/STAFF time-domain measurements at 1 AU, we show that turbulence at kinetic scales is dominated by coherent structures in the form of magnetic vortices (or current filaments), similar to what is observed in the inertial range of the solar wind turbulence and in usual fluid turbulence.

II. SPECTRUM OF THE KINETIC PLASMA TURBULENCE

To check whether the magnetic spectrum at kinetic scales displays a general shape independent of the distance R from the Sun, we have analysed 246543 individual magnetic spectra of Helios-1/SCM for radial distances $R \in [0.3, 0.9]$ AU. These spectra satisfy signal-to-noise ratios (SNR) of 2 up to 100 Hz. Among them, about 2% of the spectra show signatures of whistler waves as in [35]. These waves are mostly present in the slow wind and their occurrence as a function of R and solar wind speed is described in [34]. The spectra with signatures of whistlers were eliminated from the present study.

At 0.3 AU, in the fast wind we do not observe any whistler waves. At this radial distance, there are 3344 spectra with $\text{SNR} > 3$ up to 316 Hz and for which it was possible to determine plasma parameters, see Fig-

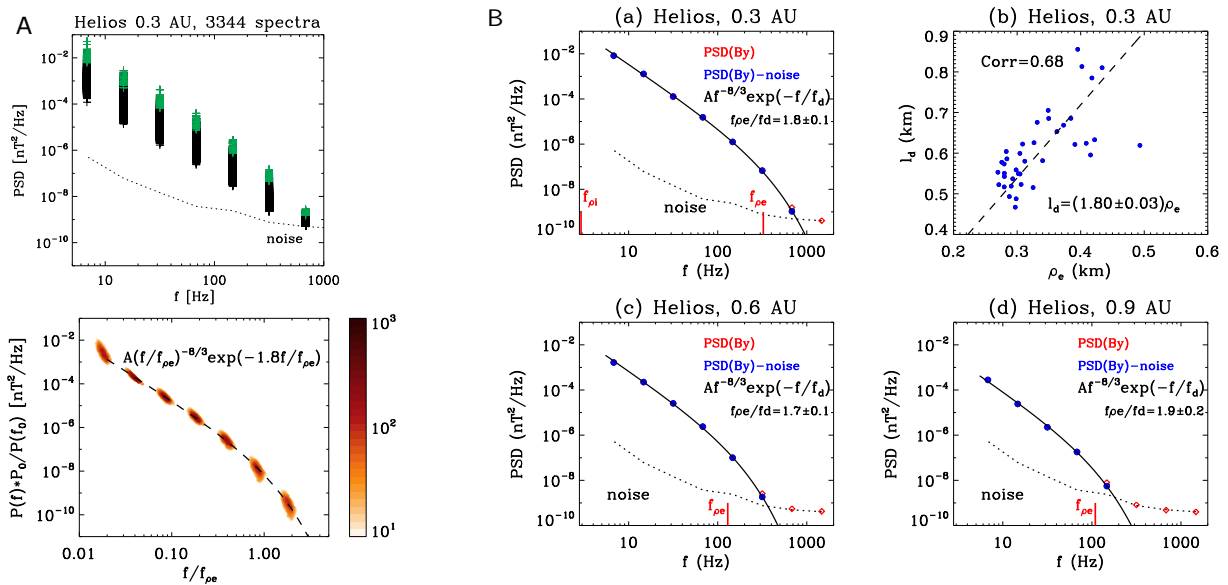


FIG. 1. A(top) 3344 individual spectra of B_y at 0.3 AU in the fast wind as measured by Helios-1/SCM; the 39 most intense spectra are marked by green crosses; SCM noise is indicated by a dotted line. A(bottom): The same 3344 spectra, but cleaned from the noise, normalised by f_{pe} and collapsed in amplitude at $\sim 0.05f/f_{pe}$; the result is shown as a 2D histogram with the number of the data points proportional to the darkness of the orange colour. The dashed line indicates the function $A(f/f_{pe})^{-8/3} \exp(-1.8f/f_{pe})$ which passes nicely through the data. B(a): One example of the most intense spectrum at 0.3 AU; the raw-spectrum is shown by red diamonds, the cleaned spectrum, after the subtraction of the noise – by blue dots; vertical red lines give the Doppler shifted ρ_p and ρ_e appearing at $f_{pp} = 2.9$ Hz and $f_{pe} = 325$ Hz respectively; black solid line gives the fit with the model function eq.(2). B(b) Results of the fitting procedure of the most intense spectra with eq.(2): dissipation scale $\ell_d = V/2\pi f_d$ as a function of the electron Larmor radius ρ_e ; the linear dependence $\ell_d = 1.8\rho_e$ is indicated by the dashed-line, with the correlation coefficient being $Corr = 0.68$. B(c) and B(d) The same as B(a) but at 0.6 and 0.9 AU respectively, at both distances, $f_{pp} \simeq 1$ Hz. At all these radial distances from the Sun, the turbulent spectrum follows the same shape $\sim f^{-8/3} \exp(-Cf/f_{pe})$, indicating independence of the solar wind expansion.

ure 1A(top). All the spectra have similar shape and they are similar to what is observed at 1 AU [3]. Among this dataset, we select the 39 most intense spectra (see green crosses in Figure 1A(top)) with $SNR > 3$ up to 681 Hz and with simultaneous measurements of \mathbf{B}_0 . One of these spectra is shown in Figure 1B(a). We performed a least square fit of these best-resolved spectra against a model with three free parameters:

$$P_{A,\alpha,f_d}: f \mapsto Af^{-\alpha} \exp(-f/f_d). \quad (1)$$

We found that the spectral index α is distributed around $8/3$, but coupled with f_d (this reflects the fact that changing α , the fitting procedure changes f_d). Moreover, the Doppler-shifted dissipation scale $\ell_d = V/2\pi f_d$ correlates with the electron Larmor radius ρ_e with a correlation coefficient of 0.6. Then, we fix $\alpha = 8/3$, and we redo the fitting of the observed spectra with the two-parameter model function:

$$P_{A,f_d}: f \mapsto Af^{-8/3} \exp(-f/f_d). \quad (2)$$

The correlation between ℓ_d and ρ_e increases slightly ($Corr \sim 0.7$) and the relation $\ell_d \sim 1.8\rho_e$ is observed, see Figure 1B(b). There is no correlation with the electron inertial length λ_e ($Corr = 0.02$, not shown). Finally, we

compare the 3344 spectra with the one-parameter model

$$P_A: f \mapsto Af^{-8/3} \exp(-1.8f/f_{pe}). \quad (3)$$

The observed spectra are well described by this model, see Figure 1A(bottom).

Further from the Sun, as expected, the intensity of the spectra decreases with R , see Figure 1B(c) and (d). Regarding the shape of the spectra, the spectral index does not change ($\alpha = 8/3$) and the dissipation frequency f_d decreases (from ~ 180 Hz at 0.3 AU to ~ 55 Hz at 0.9 AU) following f_{pe} . These observations, namely the spectral shape and the correlation between f_d and f_{pe} , agree with our results at 1 AU [3]. Thus, the turbulent spectrum at plasma kinetic scales follows the same shape at different radial distances from the Sun and it is not sensitive to the solar wind expansion, at least between 0.3 and 1 AU.

There are only few theoretical and numerical studies showing turbulent spectrum with an exponential roll-off at electron scales [27, 47, 56]. The gyrokinetic model of Howes et al. [27] assumes a critically balanced kinetic turbulence and the dissipation on the electrons via Landau damping. A similar approach is chosen in the analytical model of Schreiner and Saur [56]. Parashar et al. [47] simulate plasma with fully kinetic PIC code. There, the

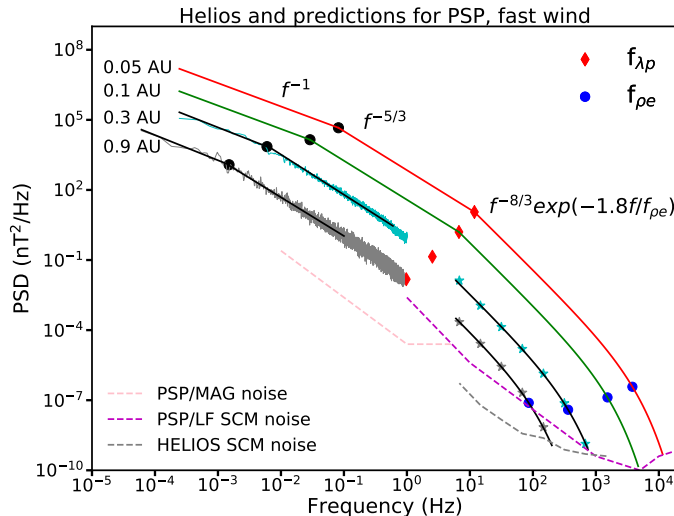


FIG. 2. The complete turbulent spectrum from energy injection scales up to the sub-electron scales at 4 radial distances from the Sun: Helios measurements at 0.9 (grey) and 0.3 AU (light blue); the predictions for the Parker Solar Probe measurements at 0.1 (green) and 0.05 AU (red). The injection scales (which correspond to $\sim f^{-1}$ spectrum) and the MHD inertial range ($\sim f^{-5/3}$) at 0.9 and 0.3 AU are covered by the Helios/MAG instrument. The Helios/SCM instrument covers the kinetic scales (stars), studied in the present paper. Dashed lines indicate noise levels of the different magnetic sensors on Helios and PSP. The Doppler shifted ion inertial length λ_p (red diamonds) marks the transition from the inertial to the kinetic range; the electron Larmor radius ρ_e (blue dots) marks the dissipation range.

spectral curvature at electron scales seems to depend on β_e , which is equivalent to the ρ_e dependency observed here.

Our results allow us to suggest a form of the turbulent kinetic spectrum which may be measured by the Parker Solar Probe (PSP) mission in the coming years, see Figure 2. This mission will be the first one approaching the Sun as close as 10 Solar Radii, i.e., ~ 0.05 AU. At such distances, the Alfvén speed is about $V_a \sim 300\text{--}1000$ km/s, [e.g., 31], and the solar wind speed becomes sub-Alfvénic, the magnetic field is very strong $B_0 \sim 10^3$ nT and plasma β (the ratio between thermal and magnetic pressures) decreases down to $\beta \sim 0.03$ [7]. If the characteristic time of the solar wind expansion remains larger than the non-linear time of the eddies at kinetic scales, the turbulent spectrum at plasma kinetic scales will follow the general shape presented here. In physical units, the dissipation will happen at much smaller scales than at 1 AU, but still around the ρ_e scale. See supplementary materials for more details.

III. NATURE OF THE KINETIC PLASMA TURBULENCE

What kind of turbulence is ‘behind’ this general spectrum? To answer this question, one needs to look at the fine structure of the fluctuations, responsible for the observed spectrum: this requires high time-

resolution measurements of kinetic scales. Unfortunately, the Helios/SCM time-domain data are not available [F. Neubauer, private communication, 2016]. Thus, the time interval we have selected for our analysis is a typical one at 1 AU from Cluster mission, and has been analysed previously at larger scales by Bale et al. [6] and Perrone et al. [49]. Here, at kinetic scales, a spectrum similar to Figure 1 is observed, see Figure 3(a). At frequencies below ~ 10 Hz, this spectrum was obtained using time series of the three components of magnetic fluctuations, as measured by Cluster/STAFF-SC in the normal mode (25 vectors per second). One of these components, $B_x(t)$ in the GSE frame, is shown on Figure 3(b) by a black line.

Figure 3(c) shows the Morlet Wavelet scalogram $W^2(t, \tau)$ [59] of $B_x(t)$, i.e., the energy distribution of the signal in time t and time-scales τ (or inversed frequencies f): it is non-homogeneously distributed with localised stalactite-like events. Such an energy distribution is usually observed in the solar wind in absence of linear instabilities, [e.g., 6, 38, 50, 52].

Figure 3(d) gives the Local Intermittency Measure (LIM),

$$I(t, \tau) = |W(t, \tau)|^2 / \langle |W(t, \tau)|^2 \rangle_t, \quad (4)$$

of the observed signal [20]. As one can see from the definition, LIM allows to see deviations of the turbulent energy from its mean at each time-scale. In this $I(t, \tau)$ -map, we observe a high number of energetic events lo-

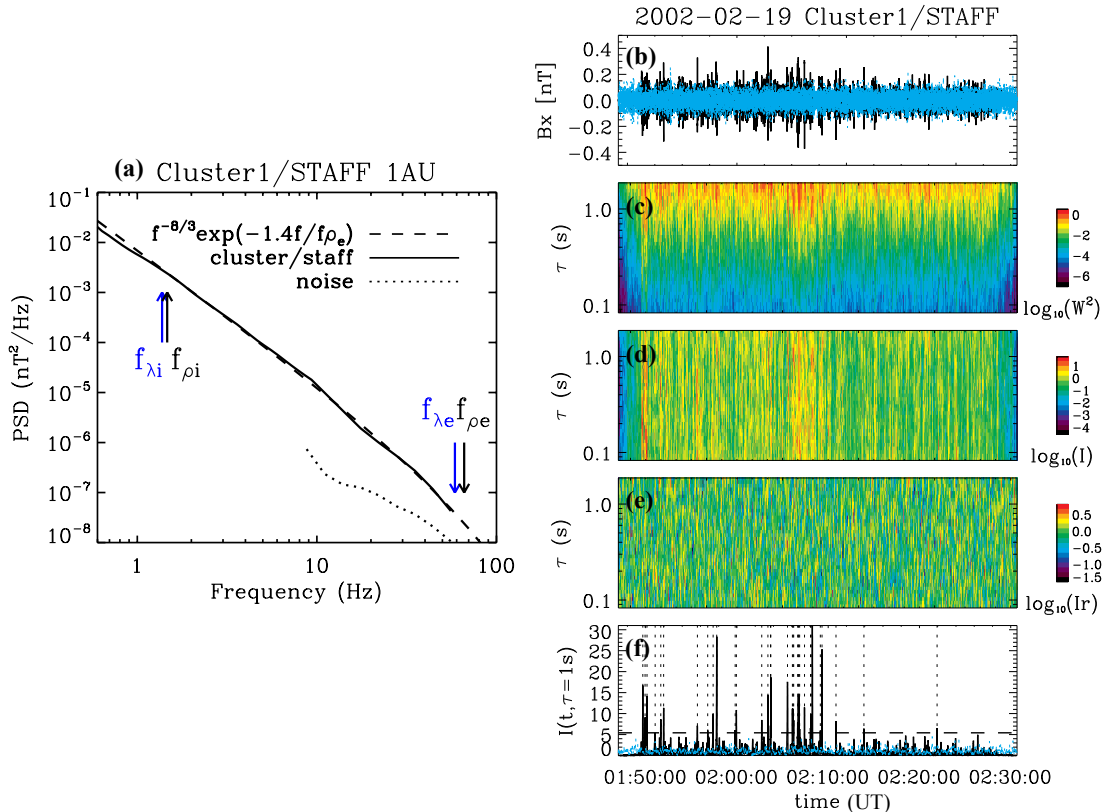


FIG. 3. (a) Spectrum of magnetic fluctuations at kinetic scales, as measured by Cluster1/STAFF at 1 AU on February 19, 2002. The ion (i.e., proton) and electron scales are indicated by arrows. The dashed line represents the fit with $\sim f^{-8/3} \exp(-1.4f/f_{\rho e})$. The dotted line is the instrumental noise. (b) The observed signal $B_x(t)$ in the GSE frame (black line), which forms the spectrum in (a), $B_{xr}(t)$ (blue line) has the same spectrum as $B_x(t)$, but random phases. (c) Wavelet scalogram $W^2(t, \tau)$ of $B_x(t)$. (d) Normalised scalogram of $B_x(t)$, $I(t, \tau)$. (e) Normalised scalogram of $B_{xr}(t)$, $I_r(t, \tau)$, in black, and $I_r(t, \tau)$, in blue, at timescale $\tau = 1$ s. There is a clear difference between the observed and the random phase signal properties: time localised energetic events delocalised in timescales, visible in panel (d) as vertical lines, are destroyed by phase randomization, see panel (e). Thus, the observed spectrum in panel (a) is primarily due to energetic events with coupled phases across scales.

calised in time and delocalised in time-scales, forming vertical lines.

What do these vertical lines in *LIM* or stalactites in the Wavelet scalogram mean? We show below that they are signatures of coherent structures, for which wavelet coefficients have coupled phases across a wide range of time-scales. For this purpose, we perform the following numerical experiment, inspired by Hada et al. [24]: we Fourier Transform $B_x(t)$, then we randomise phases keeping the amplitudes unchanged, then we do the inverse Fourier Transform and get a random-phase signal

$B_{xr}(t)$. This random phase signal is shown by the blue line on Figure 3(b) and its intermittency measure map, $I_r(t, \tau)$, in panel (e). One can see that the phase randomisation in the original signal destroys the extreme events in the time domain (panel b) and randomises the energy in the (t, τ) -plane (panel e): one does no longer observe the vertical lines in *LIM*, corresponding to short duration energetic events, covering a wide range of time-scales. This leads us to conclude that all time localised and scale delocalised energetic events, observed in Figure 3(d) have phases which are coupled across a wide

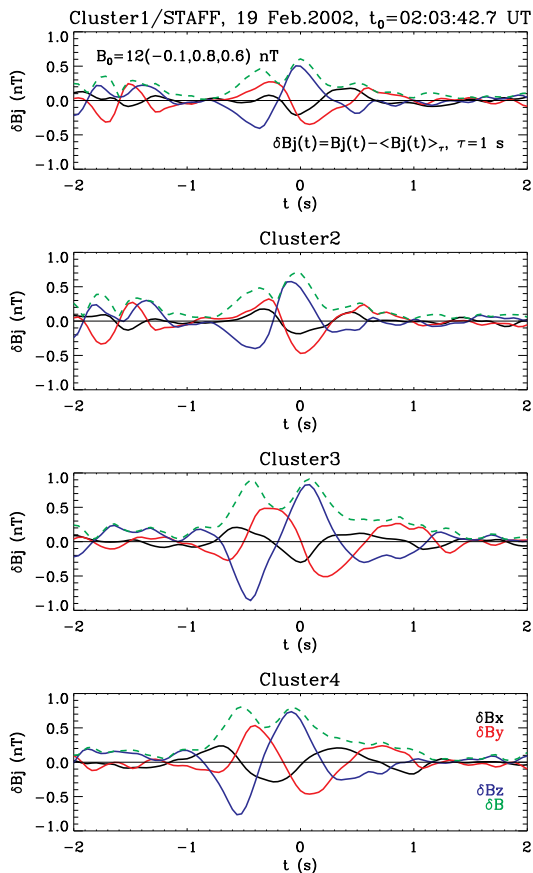


FIG. 4. A vortex-like structure at sub-ion scales observed by the 4 Cluster satellites with inter-separation distances of about 200 km, during the time interval of Figure 3. Magnetic field components are in the GSE frame. Such magnetic fluctuations correspond to current filaments localised in the centre of each structure with a cross section of the order of ion scales.

range of scales. Figure 4 shows magnetic fluctuations around such an event observed by the 4 satellites of Cluster (see the 4 panels): in the centre of the 4s-time interval we find coherent high amplitude fluctuations. The time delays between the satellites are consistent with a space localised cylindrical magnetic vortex at spatial scales of the order of the inter-satellite separations and which slightly propagates ($\sim 0.4V_a$) in the plasma frame quasi-perpendicularly to \mathbf{B}_0 . The difference of amplitude of the fluctuations detected by different satellites indicates that the 4 satellites crossed the vortex with slightly different trajectories, which confirms the space localisation of the structure. Similar vortices but at larger scales were previously observed by Alexandrova et al. [1], Perrone et al. [49, 50], Roberts et al. [52].

During the typical time interval presented on Figures 3 and 4, the Cluster satellites were 200 km apart and Cluster/STAFF measures magnetic fluctuations with 0.04 s time resolution. Such measurements allow to observe ion

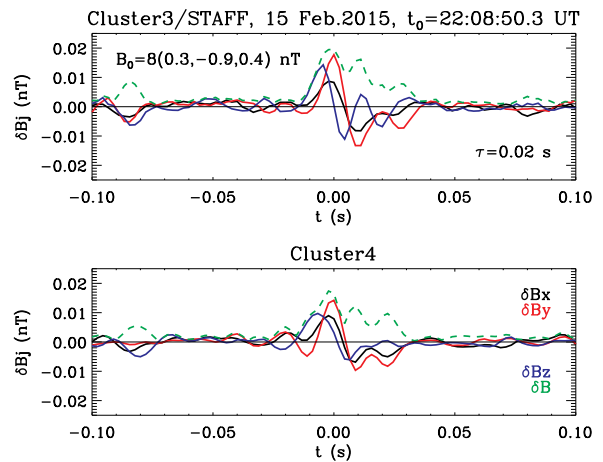


FIG. 5. Electron scale vortex-like structure crossed by 2 satellites of Cluster 7 km apart (Cluster Guest Investigator Operations); here the time interval is 20 times shorter than in Figure 4. Such magnetic fluctuations correspond to current filaments with a cross section of the order of several ρ_e .

and sub-ion scales but not electron scales. To resolve electron scales, we consider the data obtained during the Cluster Guest Investigator campaign of O. Alexandrova (2015-2016) [45]. The only available data in the free solar wind during this campaign is in the slow wind ($V \simeq 330$ km/s) on February 15, 2015. This time interval looks like any other typical solar wind turbulence, but here Cluster 3 (C3) and Cluster 4 (C4) were only 7 km apart, and the time resolution is 0.0028s (i.e., 360 vectors per second), which allows to resolve electron scales in space and in time simultaneously. We repeat the above wavelet analysis on this time interval (not shown). It reveals results similar to Figure 3 in terms of non-homogeneous distribution of turbulence energy in the (t, τ) -plane with energetic events localised in time and delocalised in time-scales, but here, up to the electron scales ($\tau \simeq 0.01$ s). The shape of the coherent structures at such small scales resembles magnetic vortices as well. An example of such an electron-scale magnetic vortex detected on 2 close satellites (C3 and C4) is shown on Figure 5: the duration of the crossing of such a vortex is about 0.05 s. The strongest gradient within this structure is localised within ~ 0.01 s, which corresponds to a spatial scale of ~ 3 km, i.e., several electron Larmor radii ρ_e . Note that this is the first time that such small-scale vortices are found in the solar wind. They can be interpreted by the theory of electron-scale vortices in high- β plasmas in the presence of an electron temperature anisotropy [30]. Similar structures have been found in 2D PIC numerical simulations [25] and in the Earth's plasma sheet [58]; bigger magnetic vortices ($\sim 30\rho_e$) have been recently detected by MMS in the Earth's magnetosheath [28].

Thus, for typical time intervals of solar wind turbu-

lence, we observe an instance of *strong turbulence* at kinetic scales, i.e., with the presence of coherent structures with coupled phases across a wide range of scales, namely, from ion to electron scales. How general are these results at 1 AU? We have analysed in the same way a dozen of hours in total in the free solar wind between 2001 and 2006 under different plasma conditions and we have always found signatures of coherent structures at kinetic scales (see another example in supplementary materials C). Then, we have done a visual check of many random samples of STAFF measurements from 19 years of Cluster mission on the Cluster Quicklook (Fields & Waves). Signatures of coherent structures, i.e., time localised and frequency delocalised energy enhancements, have been always present in the spectrograms while Cluster is in the free solar wind. Thus, it seems that *strong turbulence* is the typical situation at kinetic scales at 1 AU. This implies that the dissipation is not expected to be homogeneous but is related to coherent structures.

The topology of the coherent structures is found here to be in the form of vortex-like filaments, like in neutral fluids and within the inertial range of the solar wind turbulence [38, 49, 50, 52]. Within the kinetic range, previously, only small scale current sheets have been found [23, 48]. An interesting task will be to estimate the filling factor of vortices and current sheets at such small scales. A larger statistical study of kinetic scale vortices in the solar wind and a possible relation with coherent structures observed within the inertial range (embedding or just continuation of the same structures) will be the subject of future studies.

Can we say that what we observe at 1 AU is typical for the Heliosphere? The first results of PSP at ~ 0.17 AU [5] show that during time intervals which measures fluctuations with $\mathbf{k} \perp \mathbf{B}_0$ (for a non-radial-field wind), the same signatures of coherent structures covering inertial and kinetic ranges are present, see Figure 3 in [5]. What is the topology of these structures closer to the Sun? How do they evolve with radial distance? What is their life-time? and how can it be taken into account by turbulence models? We will address these questions in future studies using Parker Solar Probe and Solar Orbiter measurements.

IV. CONCLUSIONS AND DISCUSSIONS

Despite important differences between collisionless plasmas and neutral fluids, we find that they develop turbulent states which present several qualitative similarities.

It was already known that at MHD scales, magnetic spectra follow the same shape $\sim k^{-5/3}$ for different radial distances from the Sun [11]. Here, we show that at smaller scales the spectrum keeps also its shape independently of the radial distance (from 0.3 to 1 AU), with an exponential fall-off reminiscent of the dissipation range of neutral fluid turbulence $\sim f^{-8/3} \exp(-f/f_d)$. We show as well that the equivalent of the Kolmogorov scale ℓ_d ,

where the dissipation of the electromagnetic cascade is expected to take place, is controlled by the electron Larmor radius ρ_e for different radial distances.

This is not a trivial result, since the electron Larmor radius is not the only characteristic length at such small scales. Closer to the Sun, the electron inertial length λ_e becomes larger than the Larmor radius ρ_e , but, as observed here, it is still with ρ_e and not with λ_e that the “dissipation” scale correlates.

A significant difference occurs here with neutral fluids turbulence. In neutral fluids, the dissipation scale ℓ_d depends on the energy injection and is much larger than the mean free path, so that the dissipation range is described within the fluid approximation. As we show here, in the solar wind between 0.3 and 1 AU, on the contrary, ℓ_d is defined by ρ_e independently of the rate of energy injection. In the vicinity of ρ_e the protons are completely kinetic and electrons start to be kinetic.

The nature of the turbulent fluctuations which form the observed spectrum, presents also some similarities with the neutral fluid turbulence situation, as we observe at 1 AU. Despite small amplitudes at kinetic scales with respect to the mean field, we find many coherent structures, which cover a wide range of scales but are localised in space. These coherent events look like magnetic vortex filaments with cross section of the order of several ρ_e , and may play a crucial role in the dissipation of the space plasma turbulent cascade.

The observed general features and similarities with the usual fluid turbulence seem to indicate that similar physical processes are likely to be universal for the whole Heliosphere and may also turn out to be universal for other astrophysical turbulent plasma environments such as the interstellar medium or magnetospheres of other stars.

V. SUPPLEMENTARY MATERIALS

A. Helios-1 spectra

Measurements of magnetic fluctuations at kinetic scales are challenging: here, the level of background turbulence is low therefore only very sensitive instruments can capture the corresponding fluctuations. The most sensitive instrument devoted to kinetic scales at the moment is the Cluster/STAFF, doing measurements at 1 AU. Approaching the Sun, the turbulence level increases and therefore even with less sensitive instruments, one may expect to observe kinetic spectrum up to electron scales.

The Helios/SCM instrument [42] provides magnetic spectra for two of three components, (B_y, B_z) and rarely (B_x, B_z) , in the Spacecraft Solar ecliptic reference frame, which is equivalent to the Geocentric Solar Ecliptic (GSE) frame. For the present study we use the spectra of B_y only. Indeed, the pre-flight noise level for the B_y spectra matches well with the post-flight noise level, that is not the case for B_z [43]. The SCM spectra are in-

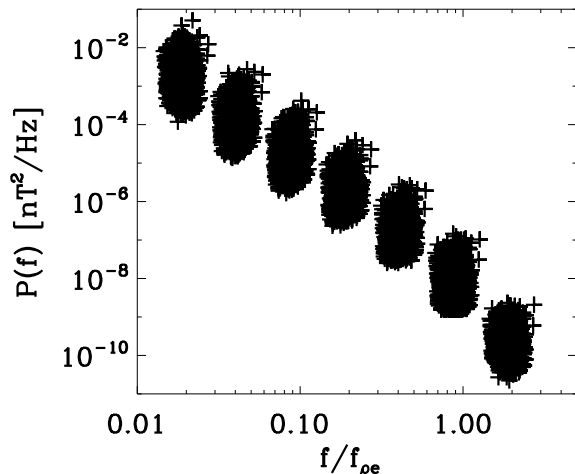


FIG. 6. The same 3344 spectra (0.3 AU) as in Figure 1A(top), but cleaned from the noise and normalised by the Doppler shifted ρ_e , f_{ρ_e} .

tegrated over 8 seconds, for 8 logarithmically spaced frequency bands, with central frequencies going from 7 Hz up to 1.5 kHz. No time domain measurements are available. Therefore, it is impossible to restore the errors on the integrated spectra over 8 seconds.

Below, we explain how Figure 1A(bottom) was obtained. As we discuss in the main body of the paper, at 0.3 AU, in the fast wind, there are 3344 spectra with signal-to-noise ratio (SNR) larger than 3 up to 316 Hz, and with plasma measurements in the close vicinity of the spectra (i.e., mean field at most within 16 seconds around the measured SCM spectrum, electron temperature within about 30 minutes and when not available, it is taken within the longer time interval from the same wind type), see Figure 1A(top). The subset of 39 most intense spectra with $\text{SNR} > 3$ up to 681 Hz and with simultaneous measurements of \mathbf{B}_0 (see green crosses in Figure 1A(top)) was used to determine two out of three free parameters of the model function $Af^{-\alpha} \exp(-f/f_d)$, namely $\alpha = -8/3$ and $f_d = f_{\rho_e}/1.8$. Now, let us verify if the established model $Af^{-8/3} \exp(-1.8f/f_{\rho_e})$ describes well the rest of the data. Figure 6 shows the same 3344 spectra as in Figure 1A(top), but here the spectra are cleaned from the noise, $P(f) = \text{PSD}(B_y) - \text{PSD}_{\text{noise}}$, and frequencies are normalised by the Doppler shifted electron Larmor radius, f_{ρ_e} . Figure 1A(bottom) shows 2D histogram calculated with the same spectra as in Figure 6 but which all pass by one point $(f_0, P_0) = (0.051, 10^{-4})$, i.e., collapsed in amplitude around $f/f_{\rho_e} = 0.051$ (the results do not change if we choose another way to collapse the spectra). The dashed line indicates the function $Af^{-8/3} \exp(-1.8f/f_{\rho_e})$, which passes through the data without any particular adjustment. Note, that the dispersion of the data points at lowest and highest frequency ends can be due to the non-simultaneous T_e measurements. Moreover, the lowest frequency can be affected

as well by the presence of the ion characteristic scales; and the highest frequencies – by the SCM noise.

Further from the Sun, the intensity of magnetic fluctuations decreases following the mean field B_0 , [e.g., 8, 10], but the kinetic scales increase (i.e., characteristic frequencies decrease) so we can resolve them with less frequency bands: At 0.6 AU, we have ~ 3000 spectra up to 147 Hz and 21 454 spectra up to 68 Hz; at 0.9 AU, there are 24 spectra with $\text{SNR} > 3$ up to 147 Hz and 10570 spectra up to 68 Hz. Their shape is still similar to what is observed at 0.3 AU.

B. Extrapolation of turbulent spectra closer to the Sun

Figure 2 of the paper shows the complete turbulent spectrum covering the energy containing scales ($\sim f^{-1}$ spectral range), the inertial range of MHD scales ($\sim f^{-5/3}$ range) and the kinetic scales, as observed at 0.3 and 0.9 AU by Helios. The most intense spectra (in green and red) are the predictions for PSP at 0.1 and 0.05 AU, respectively. For this, we assume that the turbulence level will increase together with the mean field, keeping $\delta B/B_0 \sim \text{const}$, as observed in the solar wind, [e.g., 8]. The onset of the Kolmogorov inertial range is assumed to start at the frequency f_b (black dots), which varies with R as $f_b = f_0(R_0/R)^{1.52}$ as is the case for the observed turbulence between 0.3 and 5 AU [11]. In the inner heliosphere, where $\beta < 1$, the end of the Kolmogorov scaling is expected to happen at the proton inertial length λ_p , [e.g., 10]. The exponential roll-off at the end of the electromagnetic cascade is defined by the local ρ_e , as we confirm in this study. To determine the Doppler shifted frequencies where λ_p and ρ_e will appear in the spectra ($f_{\lambda_p} = V/2\pi\lambda_p$ and $f_{\rho_e} = V/2\pi\rho_e$), we use plasma parameters (density n , electron temperature T_e , magnetic field B_0 and solar wind speed V) extrapolated from the in-situ Helios measurements (from 0.3 to 0.9 AU) [Maksimovic et al., in preparation]. More precisely these latter extrapolations have been performed by connecting the gradient of the Helios density measurements to the one measured remotely from coronal white light eclipse observations. In addition, the bulk speed profiles have been obtained by imposing the conservation of mass flux all the way down to one solar radius. The plasma parameters used for the predicted spectra as well as for the time intervals of the Helios measurements are summarized in Table 1.

It is possible that we overestimate the predicted spectrum at 0.05 AU. In fact, in the Heliosphere, $\delta B/B_0$ is of the order of unity at the largest scales of the cascade, around f_b [39]. But close to the Alfvén point (where $V = V_a$) in the vicinity of 0.05 AU, this ratio is expected to be of the order of 0.3 [60]. Therefore, the spectrum can be about one order of magnitude lower than presented here. In the coming years, PSP measurements close to the Sun will show how the empirical picture of

TABLE I. Mean plasma parameters at 4 radial distances from the Sun, corresponding to the spectra in Figure 2.

| | 0.9 AU | 0.3 AU | 0.1 AU | 0.05 AU |
|----------------------|-----------------|-----------------|--------|---------|
| B_0 (nT) | 7 ± 2 | 41 ± 3 | 280 | 990 |
| V (km/s) | 705 ± 35 | 650 ± 40 | 510 | 410 |
| N (cm $^{-3}$) | 4 ± 1 | 31 ± 4 | 350 | 1700 |
| T_p (eV) | 21 ± 5 | 50 ± 9 | 120 | 230 |
| T_e (eV) | 9 ± 2 | 15 ± 2 | 19 | 25 |
| $T_{p\perp}$ (eV) | 24 ± 5 | 65 ± 10 | - | - |
| $T_{e\perp}$ (eV) | 7 ± 1 | 12 ± 1 | - | - |
| β_p | 0.8 ± 0.2 | 0.5 ± 0.1 | 0.2 | 0.15 |
| β_e | 0.2 ± 0.1 | 0.10 ± 0.02 | 0.04 | 0.02 |
| λ_p (km) | 108 ± 14 | 39 ± 3 | 12 | 6 |
| ρ_p (km) | 101 ± 31 | 28 ± 3 | 6 | 2 |
| λ_e (km) | 2.5 ± 0.3 | 0.9 ± 0.1 | 0.3 | 0.1 |
| ρ_e (km) | 1.3 ± 0.4 | 0.3 ± 0.02 | 0.05 | 0.02 |
| f_{cp} (Hz) | 0.10 ± 0.03 | 0.6 ± 0.05 | 4 | 15 |
| $f_{\lambda p}$ (Hz) | 1.0 ± 0.1 | 2.6 ± 0.3 | 7 | 12 |
| f_{pp} (Hz) | 1.1 ± 0.3 | 3.6 ± 0.5 | 14 | 30 |
| $f_{\lambda e}$ (Hz) | 44 ± 6 | 110 ± 10 | 300 | 500 |
| f_{pe} (Hz) | 90 ± 30 | 360 ± 40 | 1530 | 3800 |
| f_{ce} (Hz) | 200 ± 60 | 1150 ± 80 | 7800 | 28000 |

the turbulence given in this article may change.

C. Signatures of coherent structures within the kinetic range: a fast wind example

The results presented in section 3 of the paper seems to be typical for solar wind turbulence at 1 AU in the absence of signatures of linear instabilities such as Alfvén Ion Cyclotron (AIC) waves at ion scales and whistler waves at electron scales. These linear waves represent only few percents of solar wind data at 1 AU [29, 35]. In the rest of the data, the typical kinetic spectrum is observed (see section 2 of the paper). For such time intervals, we usually observe signatures of intermittent coherent structures, i.e., the wavelet decomposition shows localised events in time and delocalised in scales. In section 3 of the paper, we have shown examples from the slow wind streams. Figure 7 gives an example of the fast wind ($V \sim 670$ km/s). Kinetic turbulent spectrum for this time interval follows the general shape and can be found in Figure 2 of [3]. Two bottom panels of Figure 7 give the wavelet scalogram and the Local Intermittency Measure (LIM) of magnetic field fluctuations in the kinetic range of scales. One observes here the same signatures of coherent structures as in the slow wind (Figure 3(c,d)): stalactites in $W^2(\tau, t)$ and vertical lines in the LIM . This is a typical picture for 1 AU. It will be interesting to verify these results with the new measurements of Parker Solar Probe and Solar Orbiter data closer to the Sun.

Acknowledgement OA, VJ and MM are supported by the French Centre National d'Etude Spatiales (CNES). OA thanks C. Lacombe and L. Matteini for discussions.

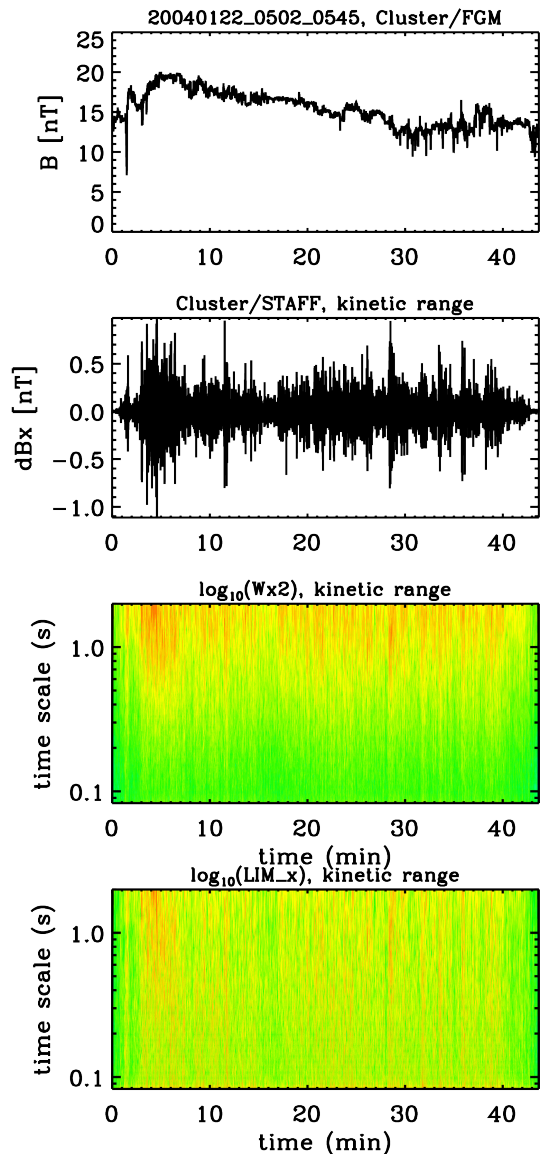


FIG. 7. Magnetic field in the fast solar wind on January 22, 2004. From up to the bottom: norm of the large scale magnetic field as measured by Cluster/FGM; B_x component of magnetic fluctuations in the GSE reference frame, within the kinetic range of scales (Cluster/STAFF-SC); Wavelet scalogram of B_x ; LIM of B_x . Vertical lines in LIM are signatures of coherent structures at kinetic scales.

Data The Helios-1 data are available on the Helios data archive (<http://helios-data.ssl.berkeley.edu/>). The Cluster data are available on the Cluster Science Archive (<https://csa.esac.esa.int/csa-web/>).

Software The Wavelet software was provided by C. Torrence and G. Compo and is available at <http://paos.colorado.edu/research/wavelets/>.

Correspondence Correspondence should be addressed to O. Alexandrova (email: olga.alexandrova@obspm.fr).

- [1] O. Alexandrova, A. Mangeney, M. Maksimovic, N. Cornilleau-Wehrlin, J.-M. Bosqued, and M. André. Alfvén vortex filaments observed in magnetosheath downstream of a quasi-perpendicular bow shock. *J. Geophys. Res.*, 111(A10):A12208, December 2006. doi:10.1029/2006JA011934.
- [2] O. Alexandrova, J. Saur, C. Lacombe, A. Mangeney, J. Mitchell, S. J. Schwartz, and P. Robert. Universality of Solar-Wind Turbulent Spectrum from MHD to Electron Scales. *Phys. Rev. Lett.*, 103(16):165003–+, October 2009. doi:10.1103/PhysRevLett.103.165003.
- [3] O. Alexandrova, C. Lacombe, A. Mangeney, R. Grappin, and M. Maksimovic. Solar Wind Turbulent Spectrum at Plasma Kinetic Scales. *ApJ*, 760:121, December 2012. doi:10.1088/0004-637X/760/2/121.
- [4] O. Alexandrova, C. H. K. Chen, L. Sorriso-Valvo, T. S. Horbury, and S. D. Bale. Solar Wind Turbulence and the Role of Ion Instabilities. *Space Sci. Rev.*, 178:101–139, October 2013. doi:10.1007/s11214-013-0004-8.
- [5] S. D. Bale, S. T. Badman, J. W. Bonnell, and journal = Nature keywords = year = "2019" month = "" volume = 576 number = eid = pages = 237-242 doi = 10.1038/s41586-019-1818-7 adsurl = adsnote = et al., title = "Highly structured slow solar wind emerging from an equatorial coronal hole".
- [6] S. D. Bale, P. J. Kellogg, F. S. Mozer, T. S. Horbury, and H. Reme. Measurement of the Electric Fluctuation Spectrum of Magnetohydrodynamic Turbulence. *Phys. Rev. Lett.*, 94(21):215002–+, June 2005. doi:10.1103/PhysRevLett.94.215002.
- [7] S. D. Bale, K. Goetz, P. R. Harvey, P. Turin, J. W. Bonnell, T. Dudok de Wit, R. E. Ergun, R. J. MacDowall, M. Pulupa, M. Andre, M. Bolton, J.-L. Bougeret, T. A. Bowen, D. Burgess, C. A. Cattell, B. D. G. Chandran, C. C. Chaston, C. H. K. Chen, M. K. Choi, J. E. Connerney, S. Cranmer, M. Diaz-Aguado, W. Donakowski, J. F. Drake, W. M. Farrell, P. Fergeau, J. Fermin, J. Fischer, N. Fox, D. Glaser, M. Goldstein, D. Gordon, E. Hanson, S. E. Harris, L. M. Hayes, J. J. Hinze, J. V. Hollweg, T. S. Horbury, R. A. Howard, V. Hoxie, G. Jannet, M. Karlsson, J. C. Kasper, P. J. Kellogg, M. Kien, J. A. Klimchuk, V. V. Krasnoselskikh, S. Krucker, J. J. Lynch, M. Maksimovic, D. M. Malaspina, S. Marker, P. Martin, J. Martinez-Oliveros, J. McCauley, D. J. McComas, T. McDonald, N. Meyer-Vernet, M. Moncuquet, S. J. Monson, F. S. Mozer, S. D. Murphy, J. Odom, R. Oliveros, J. Olson, E. N. Parker, D. Pankow, T. Phan, E. Quataert, T. Quinn, S. W. Ruplin, C. Salem, D. Seitz, D. A. Sheppard, A. Siy, K. Stevens, D. Summers, A. Szabo, M. Timofeeva, A. Vaivads, M. Velli, A. Yehle, D. Werthimer, and J. R. Wygant. The FIELDS Instrument Suite for Solar Probe Plus. Measuring the Coronal Plasma and Magnetic Field, Plasma Waves and Turbulence, and Radio Signatures of Solar Transients. *Space Sci. Rev.*, 204:49–82, December 2016. doi:10.1007/s11214-016-0244-5.
- [8] H. J. Beinroth and F. M. Neubauer. Properties of whistler mode waves between 0.3 and 1.0 AU from HELIOS observations. *J. Geophys. Res.*, 86:7755–7760, September 1981. doi:10.1029/JA086iA09p07755.
- [9] S. Boldyrev. On the Spectrum of Magnetohydrodynamic Turbulence. *ApJ*, 626:L37–L40, June 2005. doi:10.1086/431649.
- [10] S. Bourouaine, O. Alexandrova, E. Marsch, and M. Maksimovic. On Spectral Breaks in the Power Spectra of Magnetic Fluctuations in Fast Solar Wind between 0.3 and 0.9 AU. *ApJ*, 749:102, April 2012. doi:10.1088/0004-637X/749/2/102.
- [11] R. Bruno and V. Carbone. The Solar Wind as a Turbulence Laboratory. *Living Reviews in Solar Physics*, 10:2, May 2013. doi:10.12942/lrsp-2013-2.
- [12] E. Camporeale and D. Burgess. The Dissipation of Solar Wind Turbulent Fluctuations at Electron Scales. *ApJ*, 730:114, April 2011. doi:10.1088/0004-637X/730/2/114.
- [13] S. S. Cerri, F. Califano, F. Jenko, D. Told, and F. Rincon. Subproton-scale Cascades in Solar Wind Turbulence: Driven Hybrid-kinetic Simulations. *ApJ*, 822:L12, May 2016. doi:10.3847/2041-8205/822/1/L12.
- [14] B. D. G. Chandran, A. A. Schekochihin, and A. Mallet. Intermittency and Alignment in Strong RMHD Turbulence. *ApJ*, 807:39, July 2015. doi:10.1088/0004-637X/807/1/39.
- [15] S. Chen, G. Doolen, J. R. Herring, R. H. Kraichnan, S. A. Orszag, and Z. S. She. Far-dissipation range of turbulence. *Physical Review Letters*, 70:3051–3054, May 1993. doi:10.1103/PhysRevLett.70.3051.
- [16] P. J. Coleman, Jr. Turbulence, Viscosity, and Dissipation in the Solar-Wind Plasma. *ApJ*, 153:371, August 1968. doi:10.1086/149674.
- [17] N. Cornilleau-Wehrlin, P. Chauveau, S. Louis, A. Meyer, J. M. Nappa, S. Perraut, L. Rezeau, P. Robert, A. Roux, C. de Villedary, Y. de Conchy, L. Friel, C. C. Harvey, D. Hubert, C. Lacombe, R. Manning, F. Wouters, F. Lefevre, M. Parrot, J. L. Pincon, B. Poirier, W. Kofman, and P. Louarn. The Cluster Spatio-Temporal Analysis of Field Fluctuations (STAFF) Experiment. *Space Sci. Rev.*, 79:107–136, January 1997. doi:10.1023/A:1004979209565.
- [18] K. U. Denskat, H. J. Beinroth, and F. M. Neubauer. Interplanetary magnetic field power spectra with frequencies from 2.4 X 10 to the -5th HZ to 470 HZ from HELIOS-observations during solar minimum conditions. *Journal of Geophysics Zeitschrift Geophysik*, 54:60–67, 1983.
- [19] C. P. Escoubet, R. Schmidt, and M. L. Goldstein. Cluster - Science and Mission Overview. *Space Sci. Rev.*, 79:11–32, January 1997. doi:10.1023/A:1004923124586.
- [20] M. Farge. Wavelet transforms and their applications to turbulence. *Annual Review of Fluid Mechanics*, 24:395–457, 1992. doi:10.1146/annurev.fl.24.010192.002143.
- [21] S. Galtier. Wave turbulence in incompressible Hall magnetohydrodynamics. *Journal of Plasma Physics*, 72:721–769, 2006. doi:10.1017/S0022377806004521.
- [22] P. Goldreich and S. Sridhar. Toward a theory of interstellar turbulence. II. Strong Alfvénic turbulence. *ApJ*, 438:763–775, January 1995. doi:10.1086/175121.
- [23] A. Greco, S. Perri, S. Servidio, E. Yordanova, and P. Veltri. The Complex Structure of Magnetic Field Discontinuities in the Turbulent Solar Wind. *ApJ*, 823:L39, June 2016. doi:10.3847/2041-8205/823/2/L39.

- [24] T. Hada, D. Koga, and E. Yamamoto. Phase coherence of MHD waves in the solar wind. *Space Sci. Rev.*, 107: 463–466, April 2003. doi:10.1023/A:1025506124402.
- [25] C. T. Haynes, D. Burgess, E. Camporeale, and T. Sundberg. Electron vortex magnetic holes: A nonlinear coherent plasma structure. *Physics of Plasmas*, 22(1):012309, January 2015. doi:10.1063/1.4906356.
- [26] P. Hellinger, A. Verdini, S. Landi, L. Franci, and L. Matteini. von Kármán-Howarth equation for Hall magnetohydrodynamics: Hybrid simulations. *Astrophys. J. Lett.*, 857:L19, 2018. doi:10.3847/2041-8213/aabc06.
- [27] G. G. Howes, J. M. Tenbarger, and W. Dorland. A weakened cascade model for turbulence in astrophysical plasmas. *Physics of Plasmas*, 18(10):102305, October 2011. doi:10.1063/1.3646400.
- [28] S. Y. Huang, F. Sahraoui, Z. G. Yuan, J. S. He, J. S. Zhao, O. Le Contel, X. H. Deng, M. Zhou, H. S. Fu, Q. Q. Shi, B. Lavraud, Y. Pang, J. Yang, D. D. Wang, H. M. Li, X. D. Yu, C. J. Pollock, B. L. Giles, R. B. Torbert, C. T. Russell, K. A. Goodrich, D. J. Gershman, T. E. Moore, R. E. Ergun, Y. V. Khotyaintsev, P.-A. Lindqvist, R. J. Strangeway, W. Magnes, K. Bromund, H. Leinweber, F. Plaschke, B. J. Anderson, and J. L. Burch. Magnetospheric Multiscale Observations of Electron Vortex Magnetic Hole in the Turbulent Magnetosheath Plasma. *ApJ*, 836:L27, February 2017. doi:10.3847/2041-8213/aa5f50.
- [29] L. K. Jian, H. Y. Wei, C. T. Russell, J. G. Luhmann, B. Klecker, N. Omid, P. A. Isenberg, M. L. Goldstein, A. Figuera-Viñas, and X. Blanco-Cano. Electromagnetic Waves near the Proton Cyclotron Frequency: STEREO Observations. *Astrophys. J.*, 786(2):123, May 2014. doi:10.1088/0004-637X/786/2/123.
- [30] D. Jovanović, O. Alexandrova, and M. Maksimović. Theory of coherent electron-scale magnetic structures in space plasma turbulence. *Phys. Scr.*, 90(8):088002, August 2015. doi:10.1088/0031-8949/90/8/088002.
- [31] J. C. Kasper, R. Abiad, G. Austin, M. Balat-Pichelin, S. D. Bale, J. W. Belcher, P. Berg, H. Bergner, M. Berthomier, J. Bookbinder, E. Brodu, D. Caldwell, A. W. Case, B. D. G. Chandran, P. Cheimets, J. W. Cirtain, S. R. Cranmer, D. W. Curtis, P. Daigneau, G. Dalton, B. Dasgupta, D. DeTomaso, M. Diaz-Aguado, B. Djordjevic, B. Donaskowski, M. Effinger, V. Florinski, N. Fox, M. Freeman, D. Gallagher, S. P. Gary, T. Gauron, R. Gates, M. Goldstein, L. Golub, D. A. Gordon, R. Gurnee, G. Guth, J. Halekas, K. Hatch, J. Heerikuisen, G. Ho, Q. Hu, G. Johnson, S. P. Jordan, K. E. Korreck, D. Larson, A. J. Lazarus, G. Li, R. Livi, M. Ludlam, M. Maksimovic, J. P. McFadden, W. Marchant, B. A. Maruca, D. J. McComas, L. Messina, T. Mercer, S. Park, A. M. Peddie, N. Pogorelov, M. J. Reinhart, J. D. Richardson, M. Robinson, I. Rosen, R. M. Skoug, A. Slagle, J. T. Steinberg, M. L. Stevens, A. Szabo, E. R. Taylor, C. Tiu, P. Turin, M. Velli, G. Webb, P. Whittlesey, K. Wright, S. T. Wu, and G. Zank. Solar Wind Electrons Alphas and Protons (SWEAP) Investigation: Design of the Solar Wind and Coronal Plasma Instrument Suite for Solar Probe Plus. *Space Sci. Rev.*, 204: 131–186, December 2016. doi:10.1007/s11214-015-0206-3.
- [32] K. H. Kiyani, K. T. Osman, and S. C. Chapman. Dissipation and heating in solar wind turbulence: from the macro to the micro and back again. *Philosophical Transactions of the Royal Society of London Series A*, 373(2041):20140155–20140155, Apr 2015. doi:10.1098/rsta.2014.0155.
- [33] A. Kolmogorov. The Local Structure of Turbulence in Incompressible Viscous Fluid for Very Large Reynolds’ Numbers. *Akademiia Nauk SSSR Doklady*, 30:301–305, 1941.
- [34] Vamsee Krishna Jagarlamudi, Olga Alexandrova, Laura Berčić, Thierry Dudok de Wit, Vladimir Krasnoselskikh, Milan Maksimovic, and Štěpán Štverák. Whistler waves and electron properties in the inner heliosphere: Helios Observations. *to be submitted to APJ*, 2020.
- [35] C. Lacombe, O. Alexandrova, L. Matteini, O. Santolík, N. Cornilleau-Wehrin, A. Mangeney, Y. de Conchy, and M. Maksimovic. Whistler Mode Waves and the Electron Heat Flux in the Solar Wind: Cluster Observations. *ApJ*, 796:5, November 2014. doi:10.1088/0004-637X/796/1/5.
- [36] C. Lacombe, O. Alexandrova, and L. Matteini. Anisotropies of the Magnetic Field Fluctuations at Kinetic Scales in the Solar Wind: Cluster Observations. *ApJ*, 848:45, October 2017. doi:10.3847/1538-4357/aa8c06.
- [37] D. Laveder, T. Passot, and P. L. Sulem. Fluid simulations of non-resonant anisotropic ion heating. *Annales Geophysicae*, 31:1195–1204, July 2013. doi:10.5194/angeo-31-1195-2013.
- [38] S. Lion, O. Alexandrova, and A. Zaslavsky. Coherent Events and Spectral Shape at Ion Kinetic Scales in the Fast Solar Wind Turbulence. *ApJ*, 824:47, June 2016. doi:10.3847/0004-637X/824/1/47.
- [39] L. Matteini, D. Stansby, T. S. Horbury, and C. H. K. Chen. On the 1/f Spectrum in the Solar Wind and Its Connection with Magnetic Compressibility. *ApJ*, 869: L32, December 2018. doi:10.3847/2041-8213/aaf573.
- [40] W. H. Matthaeus, S. Servidio, and P. Dmitruk. Comment on “Kinetic Simulations of Magnetized Turbulence in Astrophysical Plasmas”. *Phys. Rev. Lett.*, 101:149501, 2008. doi:10.1103/PhysRevLett.101.149501.
- [41] Y. Narita, R. Nakamura, W. Baumjohann, K.-H. Glassmeier, U. Motschmann, B. Giles, W. Magnes, D. Fischer, R. B. Torbert, C. T. Russell, R. J. Strangeway, J. L. Burch, Y. Nariyuki, S. Saito, and S. P. Gary. On Electron-scale Whistler Turbulence in the Solar Wind. *ApJ*, 827:L8, August 2016. doi:10.3847/2041-8205/827/1/L8.
- [42] F. M. Neubauer, H. J. Beinroth, H. Barnstorf, and G. Dehmel. Initial results from the Helios-1 search-coil magnetometer experiment. *Journal of Geophysics Zeitschrift Geophysik*, 42:599–614, 1977.
- [43] F. M. Neubauer, G. Musmann, and G. Dehmel. Fast magnetic fluctuations in the solar wind - HELIOS I. *J. Geophys. Res.*, 82:3201–3212, August 1977. doi:10.1029/JA082i022p03201.
- [44] Note1. Satellite measurements are time series. Thus, in Fourier space one gets frequency spectra. As far as any characteristic plasma velocity, except whistlers waves phase speed, is less than the solar wind speed V , one can invoke the Taylors hypothesis and convert a spacecraft-frame frequency f to a flow-parallel wavenumber k in the plasma frame $k = 2\pi f/V$.
- [45] Note2. See <http://sci.esa.int/cluster/55616-guest-investigator-operations-2015-2016/>.
- [46] E. Papini, L. Franci, S. Landi, A. Verdini, L. Matteini, and P. Hellinger. Can Hall magnetohydrodynamics ex-

- plain plasma turbulence at sub-ion scales? *Astrophys. J.*, 870:52, 2019. doi:10.3847/1538-4357/aaf003.
- [47] Tulasi N. Parashar, William H. Matthaeus, and Michael A. Shay. Dependence of Kinetic Plasma Turbulence on Plasma β . *Astrophys. J. Lett.*, 864:L21, 2018. doi:10.3847/2041-8213/aadb8b.
- [48] S. Perri, M. L. Goldstein, J. C. Dorelli, and F. Sahraoui. Detection of Small-Scale Structures in the Dissipation Regime of Solar-Wind Turbulence. *Physical Review Letters*, 109(19):191101, November 2012. doi:10.1103/PhysRevLett.109.191101.
- [49] D. Perrone, O. Alexandrova, A. Mangeney, M. Maksimovic, C. Lacombe, V. Rakoto, J. C. Kasper, and D. Jovanovic. Compressive Coherent Structures at Ion Scales in the Slow Solar Wind. *ApJ*, 826:196, August 2016. doi:10.3847/0004-637X/826/2/196.
- [50] D. Perrone, O. Alexandrova, O. W. Roberts, S. Lion, C. Lacombe, A. Walsh, M. Maksimovic, and I. Zouganelis. Coherent Structures at Ion Scales in Fast Solar Wind: Cluster Observations. *ApJ*, 849(1):49, Nov 2017. doi:10.3847/1538-4357/aa9022.
- [51] O. W. Roberts, X. Li, and B. Li. Kinetic Plasma Turbulence in the Fast Solar Wind Measured by Cluster. *ApJ*, 769:58, May 2013. doi:10.1088/0004-637X/769/1/58.
- [52] O. W. Roberts, X. Li, O. Alexandrova, and B. Li. Observation of an MHD Alfvén vortex in the slow solar wind. *Journal of Geophysical Research (Space Physics)*, 121:3870–3881, May 2016. doi:10.1002/2015JA022248.
- [53] O. W. Roberts, O. Alexandrova, P. Kajdič, L. Turc, D. Perrone, C. P. Escoubet, and A. Walsh. Variability of the Magnetic Field Power Spectrum in the Solar Wind at Electron Scales. *ApJ*, 850:120, December 2017. doi:10.3847/1538-4357/aa93e5.
- [54] F. Sahraoui, M. L. Goldstein, G. Belmont, P. Canu, and L. Rezeau. Three Dimensional Anisotropic k Spectra of Turbulence at Subproton Scales in the Solar Wind. *Phys. Rev. Lett.*, 105:131101+, September 2010.
- [55] F. Sahraoui, S. Y. Huang, G. Belmont, M. L. Goldstein, A. Réтино, P. Robert, and J. De Patoul. Scaling of the Electron Dissipation Range of Solar Wind Turbulence. *ApJ*, 777:15, November 2013. doi:10.1088/0004-637X/777/1/15.
- [56] A. Schreiner and J. Saur. A Model for Dissipation of Solar Wind Magnetic Turbulence by Kinetic Alfvén Waves at Electron Scales: Comparison with Observations. *ApJ*, 835:133, February 2017. doi:10.3847/1538-4357/835/2/133.
- [57] Š. Štverák, P. Trávníček, M. Maksimovic, E. Marsch, A. Fazakerley, and E. E. Scime. Electron temperature anisotropy constraints in the solar wind. *J. Geophys. Res.*, 113:A03103, 2008. doi:10.1029/2007JA012733.
- [58] T. Sundberg, D. Burgess, and C. T. Haynes. Properties and origin of subproton-scale magnetic holes in the terrestrial plasma sheet. *Journal of Geophysical Research (Space Physics)*, 120:2600–2615, April 2015. doi:10.1002/2014JA020856.
- [59] C. Torrence and G. P. Compo. A Practical Guide to Wavelet Analysis. *Bulletin of the American Meteorological Society*, 79:61–78, January 1998. doi:10.1175/1520-0477(1998)079<0061:APGTWA>2.0.CO;2.
- [60] A. Verdini and M. Velli. Alfvén Waves and Turbulence in the Solar Atmosphere and Solar Wind. *ApJ*, 662:669–676, June 2007. doi:10.1086/510710.